CNS Neuroscience & Therapeutics

ORIGINAL ARTICLE

CNS Neuroscience & Therapeutics

Effect of Tacrine-3-caffeic Acid, A Novel Multifunctional Anti-Alzheimer's Dimer, Against Oxidative-Stress-Induced Cell Death in HT22 Hippocampal Neurons: Involvement of Nrf2/HO-1 Pathway

Xiao-Juan Chao,[1,†] Zi-Wei Chen,[1] An-Min Liu,[2] Xi-Xin He,[3] Shao-Gui Wang,[1] Yu-Ting Wang,[1] Pei-Qing Liu,[1] Charles Ramassamy,[4] Shing-Hung Mak,[5] Wei Cui,[5] Ah-Ng Kong,[6] Zhi-Ling Yu,[7] Yi-Fan Han[5,8] & Rong-Biao Pi[1]

1 Department of Pharmacology & Toxicology, School of Pharmaceutical Sciences, Sun Yat-Sen University, Guangzhou, China
2 Department of Neurosurgery, Sun Yat-Sen Memorial Hospital, Sun Yat-Sen University, Guangzhou, China
3 Department of Traditional Chinese Medicine Chemistry, College of Chinese Materia Madica, Guangzhou University of Chinese Medicine, Guangzhou, China
4 INRS-Institut Armand Frappier, Laval, QC, Canada
5 Department of Applied Biology and Chemical Technology, Hong Kong Polytechnic University, Hong Kong, China
6 Department of Pharmaceutics, Ernest Mario School of Pharmacy, Rutgers, The State University of New Jersey, Piscataway, NJ, USA
7 Research & Development Division, School of Chinese Medicine, Hong Kong Baptist University, Hong Kong, China
8 State Key Laboratory of Chinese Medicine and Molecular Pharmacology (Incubation), Hong Kong Polytechnic University, Shenzhen, China

Keywords
Cell death; HO-1; Nrf2; Oxidative stress; T3CA.

Correspondence
Rong-Biao Pi, Department of Pharmacology & Toxicology, School of Pharmaceutical Sciences, Sun Yat-Sen University, Guangzhou 510006, China.
Tel.: +86-20-3994-3122;
Fax: +86-20-3994-3122;
E-mail: pirb@mail.sysu.edu.cn
Received 9 February 2014; revision 23 April 2014; accepted 24 April 2014

doi: 10.1111/cns.12286

[†]Research and Development Division, School of Chinese Medicine, Hong Kong Baptist University, Hong Kong, China

The first two authors contributed equally to this work.

SUMMARY

Aims: Oxidative stress (OS) plays an important role in the pathogenesis of neurodegenerative diseases, including Alzheimer's disease (AD). This study was designed to uncover the cellular and biochemical mechanisms underlying the neuroprotective effects of tacrine-3-caffeic acid (T3CA), a novel promising multifunctional anti-Alzheimer's dimer, against OS-induced neuronal death. **Methods and Results:** T3CA protected HT22 cells against high-concentration-glutamate-induced cell death in time- and concentration-dependent manners and potently attenuated glutamate-induced intracellular reactive oxygen species (ROS) production as well as mitochondrial membrane-potential ($\Delta\Psi$) disruption. Besides, T3CA significantly induced nuclear factor erythroid 2-related factor 2 (Nrf2) nuclear translocation and increased its transcriptional activity, which were demonstrated by Western blotting, immunofluorescence, and antioxidant response element (ARE)-luciferase reporter gene assay. Further studies showed that T3CA potently up-regulated heme oxygenase-1 (HO-1), an endogenous antioxidative enzyme and a downstream effector of Nrf2, at both mRNA and protein levels. The neuroprotective effects of T3CA were partially reversed by brusatol, which reduced protein level of Nrf2, or by inhibiting HO-1 with siRNA or ZnPP-IX, a specific inhibitor of HO-1. **Conclusions:** Taken together, these results clearly demonstrate that T3CA protects neurons against OS-induced cell death partially through Nrf2/ARE/HO-1 signaling pathway, which further supports that T3CA might be a promising novel therapeutic agent for OS-associated diseases.

Introduction

Oxidative stress (OS) is an inevitable by-product of cellular respiration, and cells adapt to increased levels of reactive oxygen species (ROS) by a series of endogenous antioxidative proteins and phase II antioxidant enzymes, such as heme oxygenase-1 (HO-1) [1]. OS has been implicated in the pathogenesis of many neurodegenerative diseases [2,3] and is recognized as one of the earliest pathological changes of Alzheimer's disease (AD) [4–6]. Treatment with antioxidants might be of benefit to reduce oxidative damage and to delay AD progress [7,8]. HO-1 is an inducible enzyme that catalyzes the rate-limiting step of free heme degradation into free iron, biliverdin, and carbon monoxide [9]. The expression of HO-1 is regulated by several

transcriptional pathways, including nuclear factor erythroid 2-related factor 2 (Nrf2) [10]. Nrf2 is a basic-leucine zipper (bZIP) transcription factor that localizes in the cytoplasm bounding to its inhibitor protein, Kelch-like ECH-associated protein 1 (Keap1) [11]. After being activated, Nrf2 disassociates from Keap1, translocates to the nucleus, and binds to the antioxidant response element (ARE) sequences in the promoter regions of a set of cytoprotective genes and activates their transcription [12]. Nrf2/ARE pathway is now considered as a therapeutic target for the treatment of many OS-associated diseases, including AD in particular [13–16].

Glutamate is a major excitatory neurotransmitter in central nervous system (CNS). At high concentrations, glutamate is neurotoxic and causes neuronal cell loss associated with acute insults and chronic neurodegenerative diseases, including AD [17]. Glutamate-induced neuronal cell death has been shown through two pathways: receptor-mediated excitotoxicity and non-receptor-mediated OS [18,19]. A glutamate/cystine antiporter but not ionotropic glutamate receptors was involved in the non-receptor-mediated OS. The glutamate/cystine antiporter is required for the delivery of cystine into neuronal cells. High concentrations of extracellular glutamate inhibit the uptake of cystine, which leads to an imbalance in cellular cysteine homeostasis, progressive depletion of glutathione (GSH), accumulation of ROS, and eventually cell death [20]. HT22 cell line is a mouse immortalized hippocampal neuronal cell line and lacks functional glutamate receptors [21]. Therefore, it was frequently used in the analysis of OS-induced neuronal cell death by exposure to high concentrations of glutamate [22].

Previously, we reported that tacrine-3-caffeic acid (T3CA, (2E)-3-(3,4-dihydroxy phenyl)-N-[3-(6-chloro-1,2,3,4-tetrahydroacridin-9-ylamino)-propyl]acrylamide) (Figure 1), a novel promising multifunctional dimer against AD, can prevent glutamate- or H_2O_2-induced cell death in HT22 cells [23]. Our present study aims to investigate the cellular and biochemical mechanisms underlying the neuroprotective effects of T3CA against OS-induced neuronal death. T3CA was found to protect neurons against glutamate-induced injury and to attenuate mitochondrial damage, at least partially, through the Nrf2/ARE/HO-1 signaling pathway.

Materials and Methods

Materials

T3CA (purity > 99.0%) was synthesized by our laboratory. Glutamate was purchased from Research Biochemicals International (Natick, MA, USA). Trypsin, 3-(4,5-dimethylthiazol-2-yl)-2,5-diphenyltetrazolium bromide (MTT), dimethyl sulfoxide (DMSO), dihydroethidium (DHE), 2′,7′-dichlorofluorescin diacetate (H_2-DCF-DA), rhodamine 123, and carbonyl cyanide 3-chlorophenylhydrazone (CCCP) were obtained from Sigma-Aldrich (St. Louis, MO, USA). ZnPP-IX was purchased from Calbiochem (San Diego, CA, USA). Brusatol was obtained from Chengdu PureChem-Standard Co., Ltd. (Chengdu, China). Fetal bovine serum (FBS) and Dulbecco's modified Eagle's medium (DMEM) were purchased from Gibco-BRL (Grand Island, NY, USA). T3CA was dissolved in DMSO as 1000-fold of final concentration and kept in −20°C without light. Glutamate was dissolved in culture medium as 20-fold of final concentration before used.

Cell Culture and Treatment

HT22 cells were maintained in DMEM containing 10% FBS and incubated at 37°C under 5% CO_2. To study the protective effect of T3CA on glutamate-induced neuronal death or effects of ZnPP-IX, an inhibitor of HO-1, cells were seeded in 96-well plates (10,000 cells/well), and 6 wells were used for each group. Cells were pretreated with T3CA for 30 min or ZnPP-IX for 1 h before exposure to glutamate unless stated otherwise. Control group was treated with 0.1% (v/v) DMSO as vehicle control.

MTT Assay and Lactate Dehydrogenase Release Assay

The cell viability was determined by MTT assay as previously described [24]. The release of lactate dehydrogenase (LDH) in the culture medium was determined using a commercially available kit (Jiancheng Biochemical, Nanjing, China), as per manufacturer's protocol. Briefly, the supernatants of each well were transferred into a 96-well microplate, and reaction mixture was added to each well for 30 min at room temperature. Optical density was measured as the LDH levels using a microplate reader (Bio-Tek, Winooski, VT, USA), and all data were represented as folds over control.

Measurement of ROS

Intracellular ROS was detected using two fluorescent dyes, H_2-DCF-DA and DHE [25,26]. After treatment, cells were washed with phosphate-buffered saline (PBS, pH 7.4) and then stained with 10 μM H_2-DCF-DA or DHE in serum-free medium for 30 min at 37°C in the dark. The cells were washed with PBS and then photographed using a fluorescence microscope (Olympus, Tokyo, Japan) or extracted with 1% Triton X-100 in PBS for 10 min at 37°C. Fluorescence was recorded with an excitation wavelength of 490 nm and an emission wavelength of 525 nm for H_2-DCF-DA or an excitation wavelength of 490 nm and an emission wavelength of 595 nm for DHE by a fluorimetric plate reader Flex Station 3 (Molecular Devices, Sunnyvale, CA, USA). Values were expressed as a percentage of the fluorescence relative to the untreated control.

Estimation of Intracellular GSH and Superoxide Dismutase Activity

GSH level and the superoxide dismutase (SOD) activity were examined as described previously using commercial assay kits (Jiancheng Biochemical, Nanjing, China) [27]. After treatment, whole-cell lysate was prepared according to manufacturer's instructions. The amount of proteins was determined using the BCA assay (Pierce, Rockford, IL, USA). GSH level and relative SOD activity were normalized with protein content, and relative SOD activity was shown as percentage of the SOD activity present in control cells.

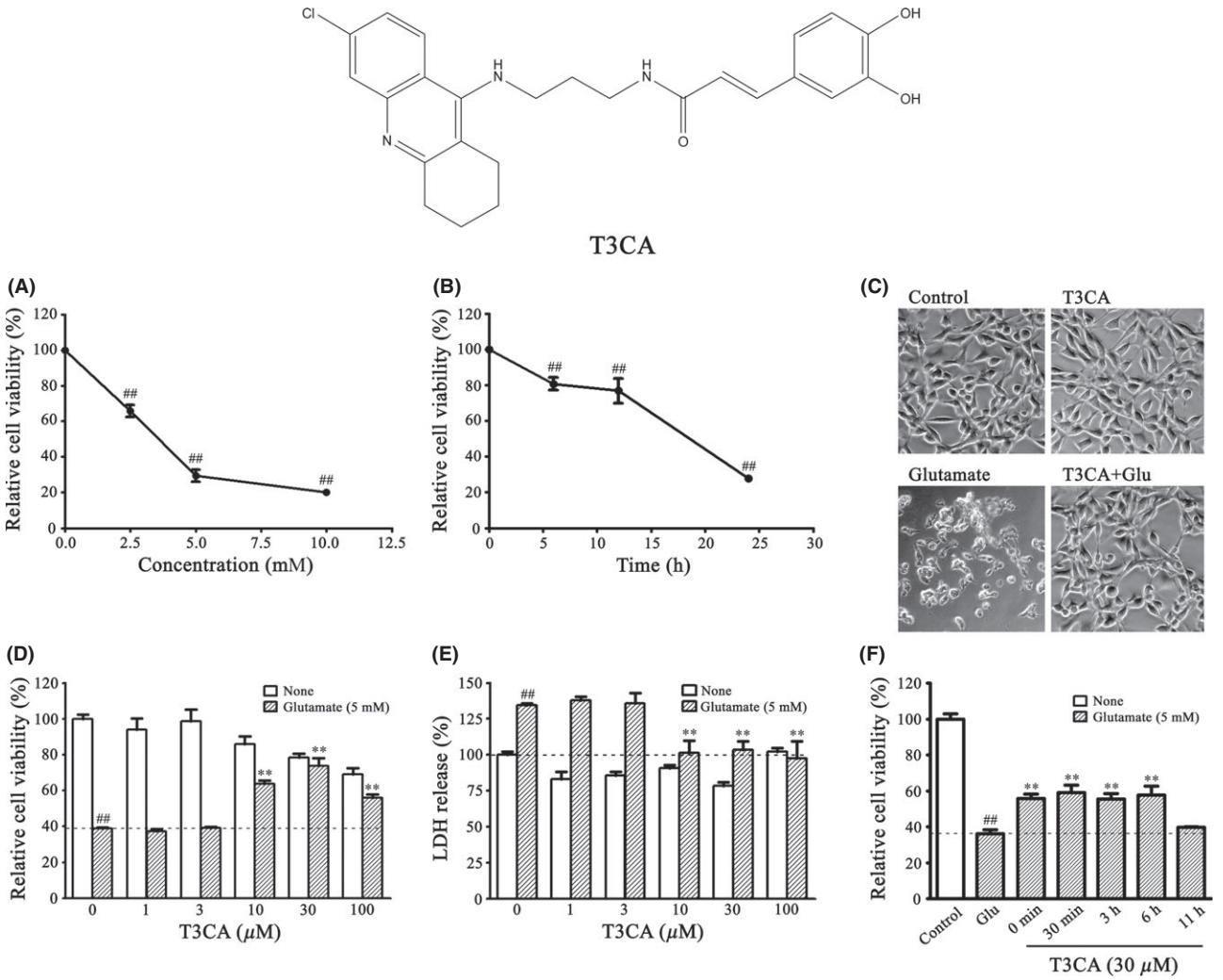

Figure 1 Chemical structure of tacrine-3-caffeic acid (T3CA) and T3CA protects HT22 cells against glutamate-induced cytotoxicity. HT22 cells were treated with glutamate at the indicated concentrations for 24 h **(A)** or with 5 mM glutamate for indicated time **(B)**. HT22 cells were photographed using a photomicroscope (×200) after cells were pretreated with/without 30 μM T3CA for 30 min and then incubated with/without 5 mM glutamate for 24 h **(C)**. HT22 cells were pretreated with/without T3CA at the indicated concentrations for 30 min and then incubated with/without 5 mM glutamate for 24 h **(D,E)**. HT22 cells were treated with 5 mM glutamate for 24 h, with/without addition of T3CA, or T3CA was added simultaneously or after the exposure to glutamate for indicated time **(F)**. Cell viability was determined using the MTT assay, and LDH release was determined using the LDH release assay. The data were represented as mean ± SD, n = 6. $^{**}P < 0.01$ versus glutamate (5 mM)-treated alone cells. $^{\#\#}P < 0.01$ versus vehicle-treated control.

Determination of Mitochondrial Membrane Potential

Rhodamine 123 was used to determine the mitochondrial membrane potential ($\Delta\Psi$) as previously reported [28]. After treatment, cells were treated with 10 μM CCCP, a mitochondrial membrane uncoupler as positive control, 5 min before staining. For fluorescence photomicrographs, cells were incubated with 5 μg/mL rhodamine 123 in PBS for 15 min at 37°C in the dark, then washed with PBS, and subjected to a laser-scanning confocal microscopy (Zeiss LSM 710, Oberkochen, Germany). For flow cytometric analysis, cells were harvested and resuspended in 1 mL PBS containing 5 μg/mL rhodamine 123. After incubating for 15 min at 37°C in the dark, cells were washed once with PBS and then analyzed using Flow Cytometer (Beckman Coulter, Brea, CA, USA); mean fluorescence intensity (MFI) of 10000 cells/sample was presented.

Mitochondrion Isolation

Mitochondria were isolated to test the cytochrome c release as described previously [29]. After treatment, cells were harvested by trypsinization and washed with ice-cold PBS. The cells were resuspended in lysis buffer (10 mM NaCl, 1.5 mM $MgCl_2$, 250 mM sucrose, 1 mM EGTA, 20 mM HEPES-KOH pH 7.4, and freshly added 1 mM DTT) with protease inhibitors' cocktails (Roche, Basel, Switzerland). Cells were manually homogenized with a motor-driven Teflon pestle homogenizer. Cell extracts were

centrifuged at 1100 *g* for 15 min at 4°C, followed by supernatant centrifugation at 15,000 *g* for 15 min at 4°C. The mitochondrial pellet was resuspended in homogenization buffer (10 mM NaCl, 1.5 mM $MgCl_2$, 250 mM sucrose, 1 mM EGTA, 20 mM HEPES-KOH pH 7.4, and freshly added 50 mM DTT) and with protease inhibitors' cocktails (Roche), and the total amount of protein was quantified using BCA assay (Pierce).

Western Blotting Analysis

Western blotting analysis was performed as previously described [30]. Nuclear and cytoplasmic extracts were isolated using Nuclear Extraction kit (Fermentas, Pittsburgh, PA, USA) and protease inhibitors' cocktails (Roche) according to the manufacturer's instructions. The antibodies used are listed in Table 1.

Immunofluorescence Staining

The nuclear distribution of Nrf2 was analyzed using immunofluorescence staining with specific antibody against Nrf2 [31]. After treatment with T3CA, HT22 cells were fixed with 4% (w/v) paraformaldehyde at room temperature for 30 min, then washed with PBS, and permeabilized in 0.1% (w/v) Triton X-100 at room temperature for 30 min followed by blocking with 10% normal goat serum (Gibco) in PBS for 1 h. The cells were incubated with primary anti-Nrf2 antibody (1:100) overnight at 4°C. After washed three times with PBS, the cells were incubated with fluorescein isothiocyanate-conjugated secondary antibody for 1 h in the dark. Stained cells were washed and photomicrographed using a laser-scanning confocal microscope (Zeiss LSM 710).

RNA Extraction and RT-PCR

Total RNA was extracted using Trizol reagent (Takara Biotechnology Co., Dalian, China) and was reverse-transcribed using One-step RT kit (Takara Biotechnology Co.) as described previously [24]. Amplification of cDNA by polymerase chain reaction was performed using Platinum Taq DNA polymerase (Takara Biotechnology Co., Dalian, China) and specific primers (Invitrogen, Shanghai, China, HO-1: forward, 5′-ACAGAAGAGGCTAAG ACCGC; reverse, 5′-TGTCAGGTATCTCCCTCCATT; *β*-actin: forward, 5′-AGCCATGTACGTAGCCATCC; reverse, 5′-CTCTCAGCT GTGGTGGTGAA). The results were obtained in 28–30 cycles of amplification. PCR products were separated by electrophoresis, visualized under UV light, and quantified by densitometric analysis using volume integration with Quantity One (Bio-Rad Laboratories, Hercules, CA, USA).

Transient Transfection and ARE-Luciferase Assay

The Dual-luciferase Reporter Assay System (Promega, Medison, WI, USA) was used to determine ARE-luciferase activity in transient transfected HT22 cells. HT22 cells were seeded in 48-wells at density of 3×10^4 per well, and 3 wells were used for each group. The ARE-driven luciferase reporter plasmid pGL6-ARE and the Renilla luciferase pRL-TK vector, used for normalization, were co-transfected into HT22 cells. Each well of cells was transfected with 200 ng of pGL6-ARE and 20 ng pRL-TK using lipofectamine 2000 (Invitrogen) according to the manufacturer's instructions. After transfection and treatment, the cell lysates were prepared with passive lysis buffer, and the firefly and Renilla luciferase activities were measured using a luminometer according to the manufacturer's instructions. Relative firefly luciferase activity was normalized to Renilla luciferase activity.

Small RNA Interference

SiRNA duplexes and nontargeting control siRNA were purchased from Jima Biotechnology (Shanghai, China). The sequences of siRNA targeting the mouse HO-1 (sense, 5′-AAGCCACACAGCA CUAUGUAAdTdT-3′; antisense, 5′-UUACAUAGU- GCUGUGUGG CUUdTdT-3′) were synthesized according to previous reports [32]. The cells were transfected at a density of ~50% confluence with siRNA duplex (50 nM) using Lipofectamine 2000 (Invitrogen). After transfection for 48 h, cells were processed for MTT assay or Western blotting analysis.

Statistical Analysis

The data were presented as the means ± standard error. Statistical analyses between two groups were performed by unpaired Stu-

Table 1 Summary of antibodies and working conditions used in the experiments

Antibody	Species	Source	Dilution
Primary antibodies			
Anti-*β*-actin	Mouse, monoclonal	Sigma-Aldrich	1:10,000
Anti-Nrf2	Rabbit, polyclonal	Santa Cruz Biotechnology Inc. CA, USA	1:500[a], 1:100[b]
Anti-HO-1	Rabbit, monoclonal	Epitomics, China	1:1000
Anti-Cytochrome C	Mouse, monoclonal	BD Biosciences, San Jose, CA, USA	1:500
Anti-Bcl 2	Rabbit, polyclonal	Santa Cruz Biotechnology Inc. CA, USA	1:1000
Anti-Keap1	Rabbit, polyclonal	Santa Cruz Biotechnology Inc.	1:300
Secondary antibodies			
Anti-Rabbit (HRP)	Goat	Santa Cruz Biotechnology Inc.	1:1000
Anti-Mouse (HRP)	Rabbit	Promega	1:10,000
Anti-Rabbit (FITC)	Goat	Santa Cruz Biotechnology Inc.	1:1000

[a]Immunoblotting. [b]Immunofluorescence.

dent's *t*-test. Differences between groups were tested by one-way analysis of variance (ANOVA). Following ANOVA, the Tukey's test was used and $P < 0.05$ was accepted to be statistically significant.

Results

T3CA Protects HT22 Cells Against Glutamate-Induced Cytotoxicity

First, the dose response and time course of glutamate-induced cell death were determined. HT22 cells were exposed to various concentrations of glutamate (2.5–10 mM) for 24 h or to 5 mM glutamate for various time periods (6–24 h), and cell viability was decreased in concentration- and time-dependent manners (Figure 1A,B). Cell viability reduced over 70% and cells became shrinkage and even debris, changing greatly in morphology after exposure to 5 mM glutamate for 24 h (Figure 1C).

T3CA alone at concentration higher than 10 μM caused a weak decrease in cell viability (MTT assay, Figure 1D), but did not increase in LDH release (Figure 2E). Pretreatment with T3CA (10-100 μM) for 30 min, followed by exposure to 5 mM glutamate, markedly attenuated glutamate-induced HT22 cell death (Figure 1C–F). T3CA (30 μM) effectively prevented HT22 cells death and reduced LDH release, both of which were induced by 5 mM glutamate. Therefore, 30 μM T3CA and 5 mM glutamate were selected for further studies to investigate the mechanism underlying T3CA's neuroprotective effect. Moreover, added simultaneously with glutamate or 30 min to 6 h after the addition of glutamate, T3CA also prevented HT22 cell death against glutamate-induced cytotoxicity (Figure 1F).

T3CA Inhibits Glutamate-Induced ROS Accumulation

To monitor the effects of T3CA on intracellular ROS level, H_2-DCF-DA and DHE staining assays were used [33]. The accumulation of ROS in HT22 cells was markedly increased by glutamate treatment, while the increase in ROS was abrogated when cells were pretreated with T3CA (Figure 2A,B). Similar results were obtained from DHE staining assay (Figure 2A,C).

Effect of T3CA on Intracellular Glutathione and SOD Levels

The exposure to glutamate for 24 h dramatically decreased intracellular GSH levels and SOD enzymatic activity. However, after pretreatment with T3CA for 30 min, intracellular GSH levels and

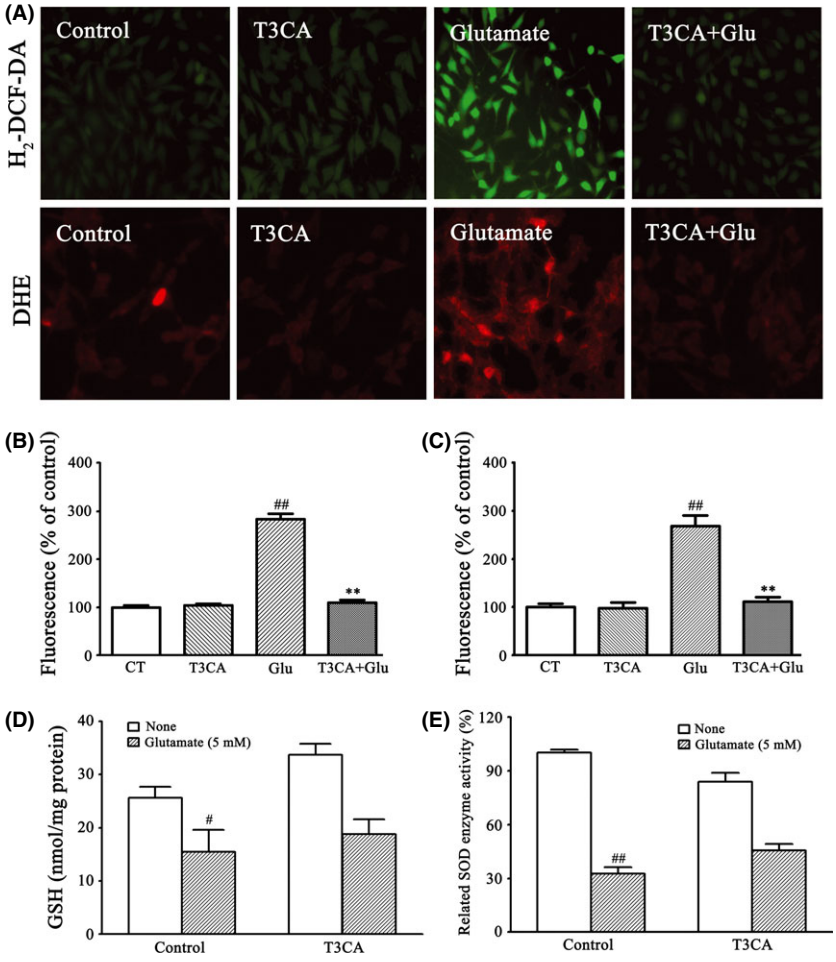

Figure 2 T3CA inhibits glutamate-induced ROS formation but does not restore the depletion of intracellular GSH and SOD enzyme activity in HT22 cells. Cells were pretreated with/without 30 μM T3CA for 30 min and then exposed to 5 mM glutamate for 12 h followed by incubation with 10 μM H2-DCF-DA **(A,B)** for 30 min or exposed to 5 mM glutamate for 16 h followed by incubation with 10 μM DHE for 30 min **(A,C)**. Cells were photographed using a fluorescence microscope (×200), and fluorescence was recorded with a fluorimetric plate reader. HT22 cells were pretreated with/without 30 μM T3CA for 30 min and then exposed to 5 mM glutamate for 24 h **(D,E)**. The SOD enzymatic activity was normalized as a ratio relative to the control activity. The data were represented as mean ± SD, n = 6. $^{**}P < 0.01$ versus glutamate-treated alone cells. $^{\#}P < 0.05$, $^{\#\#}P < 0.01$ versus vehicle-treated control.

SOD enzymatic activity were slightly increased, but no significant changes were found ($P > 0.05$, Figure 2D,E).

T3CA Protects Mitochondrial Damage

Glutamate exposure significantly hyperpolarizes the mitochondrial membrane and causes mitochondrial disruption [29]. FACS analysis and photomicrograph of the mitochondria using rhodamine 123 showed that green fluorescence significantly increased while cells were exposed to positive control CCCP, a mitochondrial membrane uncoupler, which could result in a fast breakdown of the mitochondrial membrane potential ($\Delta\Psi$) [34]. A similar shift was detected when glutamate was applied while pretreatment with T3CA blocked it (Figure 3A,B). To further study the consequences of glutamate-induced loss of $\Delta\Psi$, we determined the release of the mitochondrial protein cytochrome c (Cyto c) into the cytosol and the expression of Bcl-2, which was capable of regulating apoptosis. Cyto c was increased in the cytosolic fraction following glutamate exposure, and it was reduced by pretreatment with T3CA. However, pretreatment of T3CA did not alter the expression of Bcl-2 (Figure 3C,D).

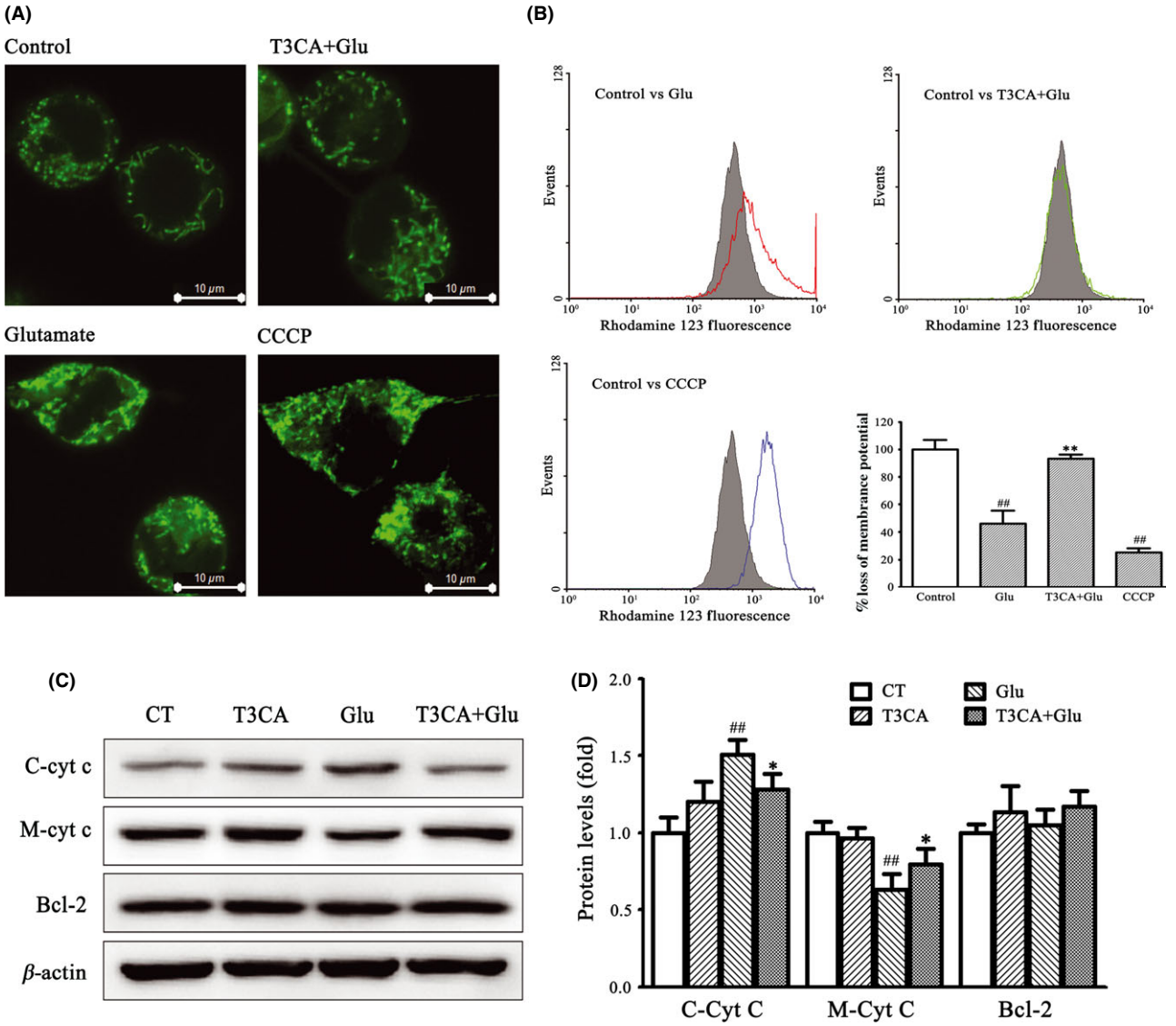

Figure 3 T3CA prevents mitochondrial damage. HT22 cells were pretreated with/without 30 μM T3CA for 30 min and then exposed to 5 mM glutamate for 12 h. Cells were then stained with the mitochondrial dye rhodamine 123 as described under Materials and methods and then photographed using laser-scanning confocal microscope **(A)** or analyzed using a flow cytometer **(B)**. CCCP (blue line) was used as positive control. Glutamate-treated group (red line) and T3CA combined with glutamate group (green line) were compared with control (solid gray). Mitochondria were isolated as described under Materials and methods. Mitochondrial proteins, cytosolic proteins, and whole cell extracts were subjected to SDS-PAGE and immunoblotting with antibodies specific to cytochrome c, Bcl-2, and β-actin as a control **(C,D)**. The bands are representative of three independent experiments. The data were represented as mean ± SD, n = 3. $^{*}P < 0.05$, $^{**}P < 0.01$ versus glutamate-treated alone cells. $^{\#\#}P < 0.01$ versus vehicle-treated control.

HO-1 Mediates T3CA's Protection

HO-1, one target gene of Nrf2, has been proposed to play an important cytodefensive role against oxidant damage. Thus, we investigated the expression of HO-1 at both mRNA and protein levels after treatment with T3CA and/or glutamate for various time periods. Treatment with 30 μM T3CA alone and the mRNA and protein levels of HO-1 were increased in a time-dependent manner within 6 and 12 h, respectively, and slightly decreased thereafter (Figure 4A,B). After treatment for 6 or 12 h, the mRNA and the protein levels of HO-1 were increased to more than 2.5-fold and 3-fold, respectively (Figure 4C,D), while after exposure to 5 mM glutamate alone for the same period, both mRNA and protein expressions of HO-1 were not altered significantly. Pretreatment with T3CA before exposure to glutamate persistently up-regulated HO-1 at both mRNA and protein levels within 12 and 24 h (Figure 4A,B).

To investigate the role of HO-1 in the protective effects of T3CA, HO-1 was either silenced by siRNA or inhibited by ZnPP-IX, an inhibitor of HO-1. Transfection with siRNA targeting HO-1 attenuated the T3CA-induced up-regulation of HO-1 (Figure 5A), while transfection with the nontargeting control (NC) siRNA did not affect the protein level of HO-1. Accordingly, silencing HO-1 reversed the protective effects of T3CA against glutamate-induced HT22 cell death (Figure 5B). Besides silencing HO-1, inhibition of HO-1 with ZnPP-IX also attenuated the protective effects of T3CA (Figure 5C).

T3CA Promotes Nrf2 Nuclear Translocation and ARE Activation

Activation of Nrf2 contributes to the up-regulation of HO-1 expression [35]. To investigate whether T3CA treatment alters the Nrf2 nucleus translocation and ARE-driven transcriptional activity in HT22 cells, multiple approaches were used. The cells were incubated with T3CA for 3–12 h at 30 μM, and the Nrf2 levels in the nuclear fractions of T3CA-treated cells showed a gradual increase, while they declined concomitantly in the cytoplasm (Figure 6A,B). Nrf2 was dramatically translocated to the nucleus after 12-h treatment (Figure 6C). Compared to that in cytoplasm, Nrf2 accumulation in nucleus increased by over fivefold in T3CA-alone-treated group and by sevenfold in T3CA-plus-glutamate-treated group (Figure 6B).

In addition, HT22 cells transiently transfected with the ARE-luciferase plasmid were exposed to T3CA, and alteration in luciferase activity was used as a measurement of ARE-driven transcription activity. The reporter assay showed that T3CA increased ARE-driven luciferase activity in a concentration-dependent manner from 3 to 30 μM (Figure 6D).

To investigate the role of Nrf2 in the up-regulation of HO-1 by T3CA and the protective effects of T3CA, brusatol was used. Brusatol was reported as a unique inhibitor of the Nrf2 pathway, which selectively reduces the protein level of Nrf2 through enhanced ubiquitination and degradation of Nrf2 [36]. Coincubation with 30 μM T3CA and 100 nM brusatol potently decreased the protein level of Nrf2 and dramatically reversed T3CA-mediated HO-1 up-regulation (Figure 6E). Accordingly, coincubation with T3CA and brusatol reversed the protective effects of T3CA against glutamate-induced HT22 cell death (Figure 6F).

T3CA Decreases Keap1 Protein Level

Under normal conditions, Nrf2 binds to Keap1, which targets Nrf2 for ubiquitin-dependent degradation in the cytoplasm and represses Nrf2-dependent gene expression [37]. After cells are exposed to reactive chemicals or OS, one or more critical cysteine residues in Keap1 can be modified, which results in degradation of Keap1, disassociation of Keap1 and Nrf2, and nuclear translocation of Nrf2 [38]. To investigate the way T3CA activates the Keap1/Nrf2/ARE pathway, the protein level of Keap1 was measured. Keap1 was potently decreased after exposure to T3CA for 1 h and was maintained in a very low level within 12 h (Figure 7).

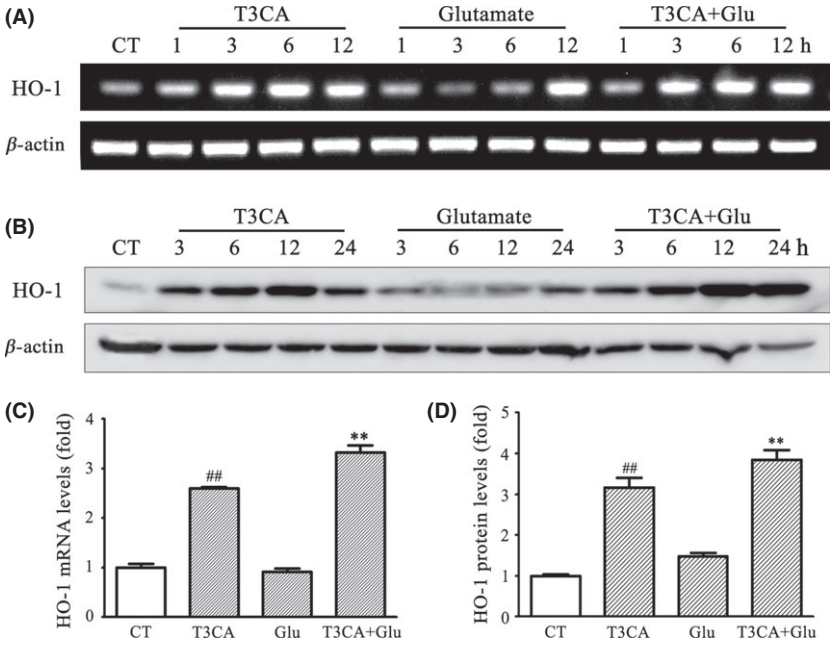

Figure 4 T3CA up-regulates HO-1. HT22 cells were pretreated with/without 30 μM T3CA for 30 min and then exposed to 5 mM glutamate for indicated time. **(A)** For RT-PCR analysis, whole mRNA extracts were subjected to RT-PCR assay, PCR products were separated by electrophoresis and visualized by UV trans-illuminator. The gels are representative of three independent experiments. **(C)** The statistics was representative of bands of control and treatment for 6-h group. **(B)** For immunoblotting assay, whole cell extracts were subjected to SDS-PAGE and immunoblotting with antibodies specific to HO-1 and β-actin as a control. The bands are representative of three independent experiments. **(D)** The statistics was representative of bands of control and treatment for 12-h group. The data were represented as mean ± SD, n = 3. $^{\#\#}P < 0.01$ versus vehicle-treated control. $^{**}P < 0.01$ versus glutamate-treated alone cells.

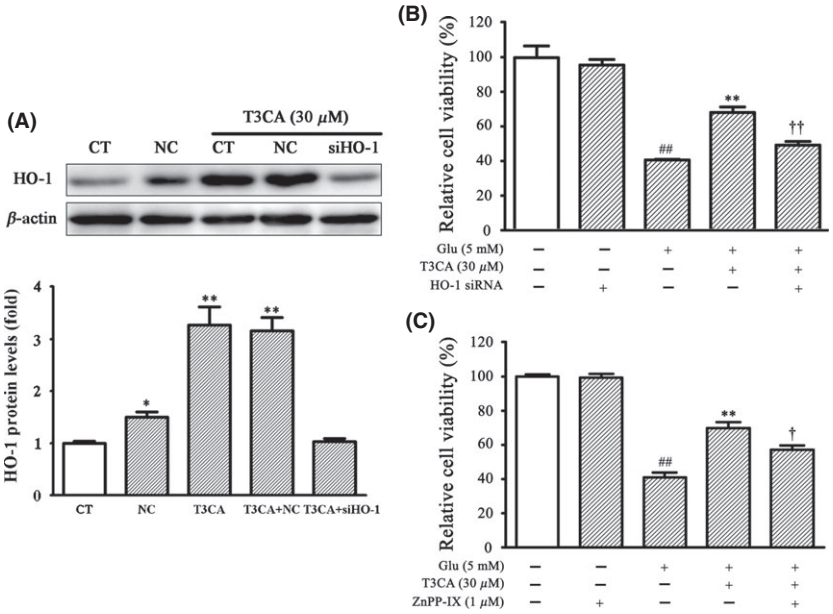

Figure 5 HO-1 mediates the protection of T3CA. HT22 cells were transfected with siRNA targeting HO-1 or negative control siRNA (NC) for 24 h and then exposed to 30 μM T3CA for 24 h **(A)** or to 30 μM T3CA for 30 min followed by exposure to 5 mM glutamate for 24 h **(B)**. For immunoblotting assay, whole cell extracts were subjected to SDS-PAGE and immunoblotting with antibodies specific to HO-1 and β-actin as a control. **(A)** The bands are representative of three independent experiments. **(B)** Cell viability was determined by the MTT assay. **(C)** Cells were pretreated with/without 1 μM ZnPP-IX for 1 h, followed by incubating with/without 30 μM T3CA for 30 min, and then exposed to 5 mM glutamate for 24 h. The data were represented as mean ± SD, n = 3. $^{\#\#}P < 0.01$ versus vehicle-treated control. $^{**}P < 0.01$ versus glutamate-treated alone cells. $^{\dagger}P < 0.05$, $^{\dagger\dagger}P < 0.01$ versus T3CA combination with glutamate-treated cells.

Discussion

Here, we demonstrated that T3CA, a novel promising multifunctional anti-AD candidate, prevented glutamate-induced cell death in HT22 cells by activating the Nrf2/ARE/HO-1 pathway, an endogenous prosurvival signaling pathway.

OS contributes to aging and age-related diseases, such as cancer, cardiovascular diseases, chronic inflammation, and neurodegenerative diseases [39]. It was recognized as one of the earliest pathological changes that occurred in the pathogenesis of AD. OS and damage are combated by endogenous antioxidant components and enzymes. However, it is reported that AD brain has significantly decreased levels of antioxidant enzymes, which causes the brain more vulnerable to oxidative damage [40]. Brain-accessible antioxidants have not only exogenous radical scavenging property, but also an ability to induce endogenous antioxidative genes that might be more helpful in the treatment for ROS-associated diseases, including AD [41].

In the present study, T3CA was found to markedly reduce glutamate-induced HT22 cell death (Figure 1D,E), which was in compliance with our previous reports [23,42]. Treatment with T3CA (30 μM) alone or combined with glutamate reduced the amount of cells, which resulted in decrease in cell viability (MTT assay) (Figure 1C,D). But it was interesting that T3CA did not increase the LDH release (Figure 1E), suggesting that T3CA (30 μM) might not be cytotoxic but only inhibit the cell proliferation [43–45]. It was reported that biophenol and polyphenols, such as caffeic acid and caffeic acid derivatives, were capable of inhibiting cell proliferation [46], suggesting that T3CA, a polyphenol, might also inhibit the proliferation of fissionable cells. Interestingly, when T3CA was added simultaneously with glutamate or 30 min to 6 h after the addition of glutamate, it still protected HT22 cells against glutamate-induced cytotoxicity (Figure 1F), suggesting that T3CA exhibited not only preventive effects but also therapeutic effects against oxidative damage with wide time windows.

We previously demonstrated that T3CA could directly scavenge DPPH free radicals [23]. Therefore, we hypothesized that T3CA could reduce the ROS accumulation within cells. T3CA significantly reduced glutamate-induced ROS generation in HT22 cells detected by using two fluorescence dyes H_2-DCF-DA and DHE (Figure 2A–C); the former is the indicator for H_2O_2, and the later one is for O_2^- [47]. It was reported that exposure to high concentration of glutamate resulted in intracellular GSH depletion, ROS accumulation, decrease in SOD activity, mitochondrial dysfunction, and cell death in HT22 cells [48]. However, our study showed that pretreatment with T3CA dramatically reduced ROS accumulation without attenuating the GSH depletion and SOD activity reduction in glutamate-treated HT22 cells (Figure 2D,E). It was reported that the depletion of GSH was necessary for the initial increase in ROS production, while GSH decrease was insufficient to generate the late ROS increase after 6 h of glutamate treatment in HT22 cells when the mitochondrial electron transport chain was the major source of ROS [49]. Moreover, the prevention of mitochondrial OS was sufficient to protect against

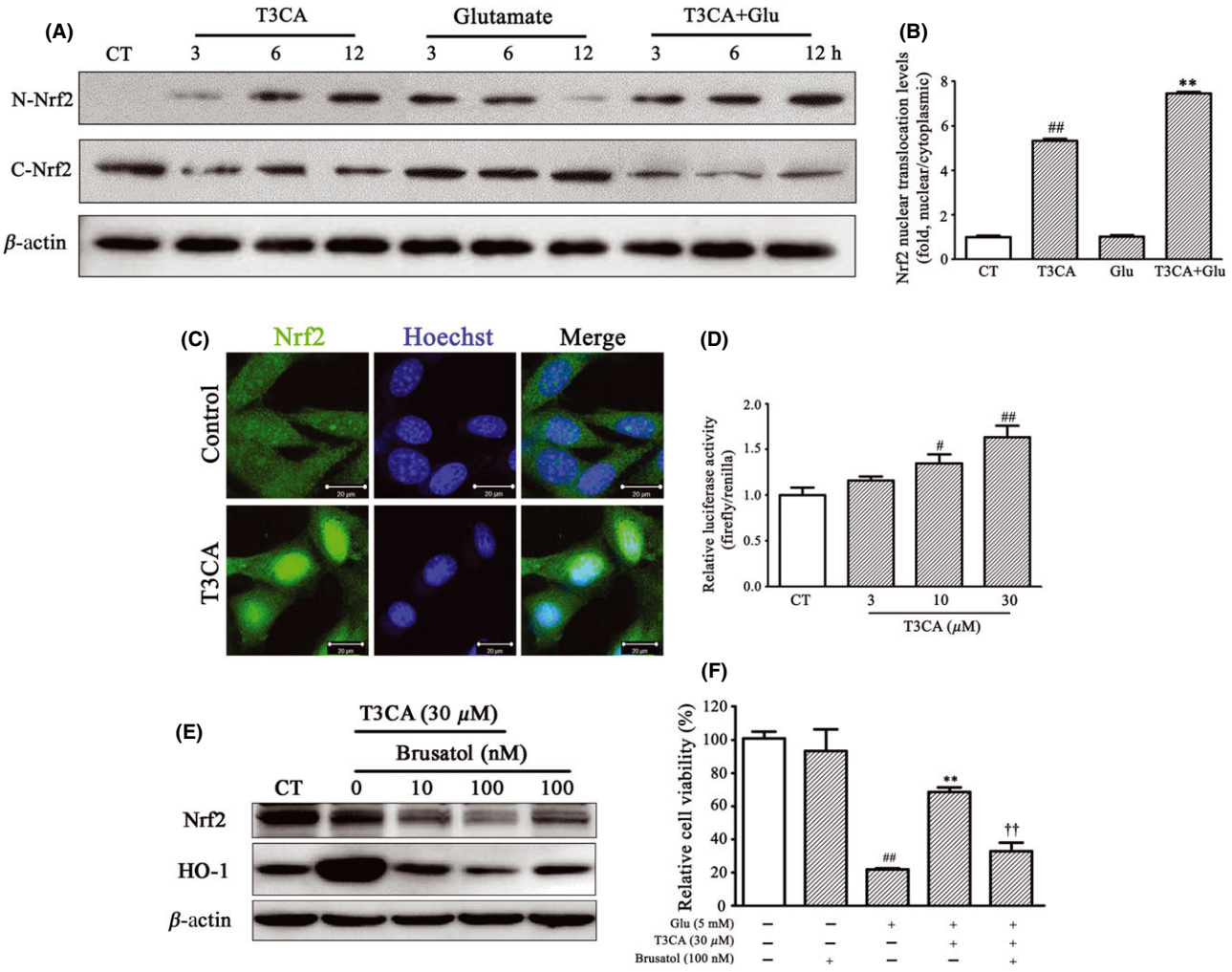

Figure 6 T3CA activates Nrf2/ARE pathway, and Nrf2 mediates the protection of T3CA. **(A)** HT22 cells were pretreated with/without 30 μM T3CA for 30 min and then exposed to 5 mM glutamate for indicated time period. Nuclear and cytoplasmic extracts were isolated as described under Materials and methods and subjected to SDS-PAGE and immunoblotting with antibodies specific to Nrf2 and β-actin as a control. **(B)** The statistics was representative of bands of control and treatment for 12-h group. **(C)** HT22 cells were treated with 30 μM T3CA for 12 h. Cells were immunofluorescence stained with anti-Nrf2 antibody. Nuclear counterstaining was carried out with Hoechst 33258. Fluorescence was visualized by a laser-scanning confocal microscope. **(D)** After 24-h transfection, cells were treated with indicated concentration T3CA for 24 h. ARE luciferase reporter gene assay was performed using a commercial kit. **(E)** Cells were pretreated with/without different concentration of brusatol for 1 h, followed by incubating with/without 30 μM T3CA for 24 h, or **(F)** for 30 min followed by exposure to 5 mM glutamate. The bands are representative of three independent experiments. Cell viability was determined by the MTT assay. $^{\#}P < 0.05$, $^{\#\#}P < 0.01$ versus vehicle-treated control. $^{**}P < 0.01$ versus glutamate-treated alone cells. $^{\dagger\dagger}P < 0.01$ versus T3CA combination with glutamate-treated cells.

glutamate-induced oxytosis in HT22 cells, and the recovery of GSH was not necessary [50]. SOD converts superoxide anion to hydrogen peroxide, which can be further detoxified. Usually, SOD responds to severe GSH depletion or OS. However, it was reported that polyphenol, such as flavonoids or caffeic acid phenethyl ester (CAPE), a caffeic acid derivative, might adjust oxidant and antioxidant balance in cell lines by reacting with oxygen free radicals and decrease the demand for endogenous O_2-scavenging antioxidants such as SOD and then protect OS-induced cell death [51]. Our results indicated that T3CA prevents OS-induced cell death through a GSH- and SOD-independent mechanism.

Increasing evidence suggested that mitochondrial dysfunction plays an important role in the pathogenesis of AD [52]. Inhibition of mitochondrial dysfunction was capable of attenuating Aβ-induced neurotoxicity in PC12 cells [53]. Several mitochondria-targeting compounds have been identified with potential efficacy in AD, such as hydroxytyrosol, curcumin, flavanols, and omega-3 polyunsaturated fatty acid [54]. Hence, the effects of T3CA on mitochondrial function were then explored. As shown in Figure 3A,B, pretreatment with T3CA stabilized mitochondrial membrane potential, the disruption of which plays a key role in early stage of mitochondrial dysfunction. Cyto c, which locates at mitochondrial inner membrane,

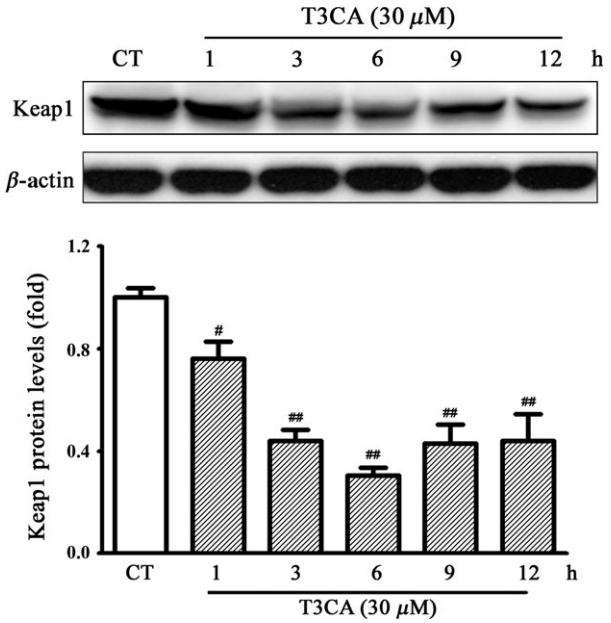

Figure 7 T3CA decreases the protein level of Keap1. HT22 cells were treated with 30 μM T3CA for indicated time period. Whole cell extracts were subjected to SDS-PAGE and immunoblotting with antibodies specific to Keap1 and β-actin as a control. The bands are representative of three independent experiments. $^{\#}P < 0.05$, $^{\#\#}P < 0.01$ versus vehicle-treated control.

was released from mitochondria in response to proapoptotic stimuli [29]. Up-regulation of Bcl-2, an antiapoptotic protein, is able to inhibit OS-induced cells death [55]. Our results showed that pretreatment with T3CA reduced glutamate-induced Cyto c release into cytosol, but not significantly up-regulated Bcl-2, which suggested that T3CA restored mitochondria function in a Bcl-2-independent manner.

Besides its exogenous radical scavenging property (DPPH free radicals scavenging assay), we wonder whether T3CA could attenuate intracellular ROS accumulation and protect OS-induced cell death further through its activation of endogenous antioxidative networks. Among these endogenous antioxidative proteins and enzymes, HO-1 is an inducible phase II antioxidant enzyme and can be up-regulated in response to multiple oxidative stimulations, such as UV light, heme, heavy metals, GSH depletion, and H_2O_2 [14]. In this study, HO-1 was found to be dramatically up-regulated by T3CA at mRNA and protein levels (Figure 4A,B). It is some surprising that silencing HO-1 by siRNA or inhibiting HO-1 by ZnPP-IX, an inhibitor of HO-1, only partially blocked the cytoprotection of T3CA (Figure 5B, C). These results suggested that the neuroprotective effect of T3CA against glutamate-induced cell death partially attributes to HO-1 in HT22 cells. HO-1 could be posttranslationally modified by phosphorylated, which does not appear to increase its catalytic activity [56]. It is clear that the main mechanism of HO-1 regulation took place at the transcriptional level [57]. Therefore, Nrf2, the main upstream transcription factor of HO-1, was explored.

Increasing evidence gave proof for the activation of Nrf2/ARE pathway as a promising target for AD treatment [58–60]. In this study, we found that T3CA increased Nrf2 nuclear translocation (Figure 6A–C). Nrf2 was also slightly translocated to nucleus in the first 3–6 h in glutamate-treated group, but it did not last after 6 h. When cells were exposed to OS, the cytoplasmic Nrf2 translocated to nucleus [61]. Moreover, the ARE-driven transcriptional activity was induced by T3CA (Figure 6D). To investigate whether Nrf2 plays a key role in the protection of T3CA, brusatol, a Keap1/Nrf2/ARE pathway inhibitor, was adopted. Brusatol decreased the protein level of Nrf2, significantly reversed the up-regulation of HO-1 by T3CA, and dramatically attenuated the protection of T3CA (Figure 6E,F).

The disassociation of Nrf2 from Keap1 may be through the direct modification of reactive cysteine residues in Keap1 by endogenous products of OS or reactive chemicals [12,62,63]. After treatment with T3CA, protein level of Keap1 was dramatically decreased (Figure 7), suggesting the degradation of Keap1. Therefore, T3CA might activate the Keap1/Nrf2/ARE pathway through directly degrading Keap1.

In summary, our findings clearly demonstrate that T3CA, a novel promising multifunctional anti-Alzheimer's dimer, prevents OS-induced neuronal death through activating the Nrf2/ARE/HO-1 pathway, an endogenous antioxidative system, indicating that T3CA appears to have significant potential in preventing OS-associated diseases, such as AD.

Acknowledgments

This research was supported by grants from Fundamental Research Funds for the Central Universities (No. 10ykpy23), Guangdong Provincial International Cooperation Project of Science & Technology (No. 2012B050300015), National Natural Science Foundation of China/RGC Hong Kong Joint Research Scheme (No. 30731160617), and Scientific and Technological Cooperation between the Italian Republic and the People's Republic of China for Year 2013-2015 (No. MAE-M00705\CN13MO9) to R. Pi, and National Natural Science Foundation of China/RGC Hong Kong Joint Research Scheme (No. N_PolyU61807) and RGC Hong Kong Research Scheme (No. PolyU5610/11M) to Y. Han.

Conflict of Interest

The authors declare no conflict of interest.

References

1. Takahashi T, Morita K, Akagi R, Sassa S. Heme oxygenase-1: a novel therapeutic target in oxidative tissue injuries. *Curr Med Chem* 2004;**11**: 1545–1561.
2. Lin M, Beal MF. Mitochondrial dysfunction and oxidative stress in neurodegenerative diseases. *Nature* 2006;**443**:787–795.
3. Valko M, Leibfritz D, Moncol J, et al. Free radicals and antioxidants in normal physiological functions and human disease. *Int J Biochem Cell Biol* 2007;**39**:44–84.
4. Nunomura A, Perry G, Aliev G, et al. Oxidative damage is the earliest event in Alzheimer disease. *J Neuropathol Exp Neurol* 2001;**60**:759–767.
5. Beal MF. Oxidative damage as an early marker of Alzheimer's disease and mild cognitive impairment. *Neurobiol Aging* 2005;**26**:585–586.

6. Smith MA, Zhu X, Tabaton M, et al. Increased iron and free radical generation in preclinical Alzheimer disease and mild cognitive impairment. *J Alzheimers Dis* 2010;**19**:363–372.
7. Di Bona D, Scapagnini G, Candore G, et al. Immune-inflammatory responses and oxidative stress in Alzheimer's disease: therapeutic implications. *Curr Pharm Des* 2010;**16**:684–691.
8. Dumont M, Beal MF. Neuroprotective strategies involving ROS in Alzheimer disease. *Free Radic Biol Med* 2011;**51**:1014–1026.
9. Willis D, Moore AR, Frederick R, Willoughby DA. Heme oxygenase: a novel target for the modulation of the inflammatory response. *Nat Med* 1996;**2**:87–90.
10. Reichard JF, Motz GT, Puga A. Heme oxygenase-1 induction by NRF2 requires inactivation of the transcriptional repressor BACH1. *Nucleic Acids Res* 2007;**35**:7074–7086.
11. Kaspar JW, Niture SK, Jaiswal AK. Nrf2:INrf2 (Keap1) signaling in oxidative stress. *Free Radic Biol Med* 2009;**47**:1304–1309.
12. Kensler TW, Wakabayashi N, Biswal S. Cell survival responses to environmental stresses via the Keap1-Nrf2-ARE pathway. *Annu Rev Pharmacol Toxicol* 2007;**47**:89–116.
13. Mulcahy RT, Wartman MA, Bailey HH, Gipp JJ. Constitutive and beta-naphthoflavone-induced expression of the human gamma-glutamylcysteine synthetase heavy subunit gene is regulated by a distal antioxidant response element/TRE sequence. *J Biol Chem* 1997;**272**:7445–7454.
14. Cuadrado A, Rojo AI. Heme oxygenase-1 as a therapeutic target in neurodegenerative diseases and brain infections. *Curr Pharm Des* 2008;**14**:429–442.
15. Hybertson BM, Gao B, Bose SK, McCord JM. Oxidative stress in health and disease: the therapeutic potential of Nrf2 activation. *Mol Aspects Med* 2011;**32**:234–246.
16. Pickering AM, Linder RA, Zhang H, Forman HJ, Davies KJ. Nrf2-dependent induction of proteasome and Pa28alphabeta regulator are required for adaptation to oxidative stress. *J Biol Chem* 2012;**287**:10021–10031.
17. Wang Y, Song JH, Denisova JV, et al. Neuronal gap junction coupling is regulated by glutamate and plays critical role in cell death during neuronal injury. *J Neurosci* 2012;**32**:713–725.
18. Choi DW. Glutamate neurotoxicity and diseases of the nervous system. *Neuron* 1988;**1**:623–634.
19. Lipton SA. Pathologically activated therapeutics for neuroprotection. *Nat Rev Neurosci* 2007;**8**:803–808.
20. Murphy TH, Miyamoto M, Sastre A, Schnaar RL, Coyle JT. Glutamate toxicity in a neuronal cell line involves inhibition of cystine transport leading to oxidative stress. *Neuron* 1989;**2**:1547–1558.
21. Maher P, Davis JB. The role of monoamine metabolism in oxidative glutamate toxicity. *J Neurosci* 1996;**16**:6394–6401.
22. Fukui M, Choi HJ, Zhu B. Mechanism for the protective effect of resveratrol against oxidative stress-induced neuronal death. *Free Radic Biol Med* 2010;**49**:800–813.
23. Chao X, He X, Yang Y, et al. Design, synthesis and pharmacological evaluation of novel tacrine-caffeic acid hybrids as multi-targeted compounds against Alzheimer's disease. *Bioorg Med Chem Lett* 2012;**22**:6498–6502.
24. Lin R, Chen X, Li W, et al. Exposure to metal ions regulates mRNA levels of APP and BACE1 in PC12 cells: blockage by curcumin. *Neurosci Lett* 2008;**440**:344–347.
25. Li B, Jeong GS, Kang DG, Lee HS, Kim YC. Cytoprotective effects of lindenenyl acetate isolated from Lindera strychnifolia on mouse hippocampal HT22 cells. *Eur J Pharmacol* 2009;**614**:58–65.
26. Vara D, Campanella M, Pula G. The novel NOX inhibitor 2-acetylphenothiazine impairs collagen-dependent thrombus formation in a GPVI-dependent manner. *Br J Pharmacol* 2013;**168**:212–224.
27. Pi R, Mao X, Chao X, et al. Tacrine-6-ferulic Acid, a novel multifunctional dimer, inhibits amyloid-beta-mediated Alzheimer's disease-associated pathogenesis *in vitro* and *in vivo*. *PLoS ONE* 2012;**7**:e31921.
28. Chazotte B. Labeling mitochondria with rhodamine 123. *Cold Spring Harb Protoc* 2011;**2011**:892–894.
29. Pallast S, Arai K, Wang X, Lo EH, van Leyen K. 12/15-Lipoxygenase targets neuronal mitochondria under oxidative stress. *J Neurochem* 2009;**111**:882–889.
30. Mao X, Yin W, Liu M, et al. Osthole, a natural coumarin, improves neurobehavioral functions and reduces infarct volume and matrix metalloproteinase-9 activity after transient focal cerebral ischemia in rats. *Brain Res* 2011;**1385**:275–280.
31. Feng R, Lu Y, Bowman LL, et al. Inhibition of activator protein-1, NF-kappaB, and MAPKs and induction of phase 2 detoxifying enzyme activity by chlorogenic acid. *J Biol Chem* 2005;**280**:27888–27895.
32. Zhang X, Shan P, Jiang D, et al. Small interfering RNA targeting heme oxygenase-1 enhances ischemia-reperfusion-induced lung apoptosis. *J Biol Chem* 2004;**279**:10677–10684.
33. Aranda A, Sequedo L, Tolosa L, et al. Dichloro-dihydro-fluorescein diacetate (DCFH-DA) assay: a quantitative method for oxidative stress assessment of nanoparticle-treated cells. *Toxicol In Vitro* 2013;**27**:954–963.
34. Lim ML, Minamikawa T, Nagley P. The protonophore CCCP induces mitochondrial permeability transition without cytochrome c release in human osteosarcoma cells. *FEBS Lett* 2001;**503**:69–74.
35. Srisook K, Kim C, Cha YN. Molecular mechanisms involved in enhancing HO-1 expression: de-repression by heme and activation by Nrf2, the "one-two" punch. *Antioxid Redox Signal* 2005;**7**:1674–1687.
36. Ren D, Villeneuve NF, Jiang T, et al. Brusatol enhances the efficacy of chemotherapy by inhibiting the Nrf2-mediated defense mechanism. *Proc Natl Acad Sci USA* 2011;**108**:1433–1438.
37. Kang KW, Lee SJ, Kim SG. Molecular mechanism of nrf2 activation by oxidative stress. *Antioxid Redox Signal* 2005;**7**:1664–1673.
38. Bryan HK, Olayanju A, Goldring CE, Park BK. The Nrf2 cell defence pathway: Keap1-dependent and -independent mechanisms of regulation. *Biochem Pharmacol* 2013;**85**:705–717.
39. Gwon AR, Park JS, Arumugam TV, et al. Oxidative lipid modification of nicastrin enhances amyloidogenic gamma-secretase activity in Alzheimer's disease. *Aging Cell* 2012;**11**:559–568.
40. Texel SJ, Mattson MP. Impaired adaptive cellular responses to oxidative stress and the pathogenesis of Alzheimer's disease. *Antioxid Redox Signal* 2011;**14**:1519–1534.
41. Pratico D. Oxidative stress hypothesis in Alzheimer's disease: a reappraisal. *Trends Pharmacol Sci* 2008;**29**:609–615.
42. Pi R, Chao X, He X, et al. Hybrids of tacrine and caffeic acid, the synthesis and combinations of drugs. C.N.Patent: CN102617465A. 2011.
43. Lobner D. Comparison of the LDH and MTT assays for quantifying cell death: validity for neuronal apoptosis? *J Neurosci Methods* 2000;**96**:147–152.
44. Denizot F, Land R. Rapid colorimetric assay for cell growth and survival. Modifications to the tetrazolium dye procedure giving improved sensitivity and reliability. *J Immunol Methods* 1986;**89**:271–277.
45. Arechabala B, Coiffard C, Rivalland P, Coiffard LJ, de Roeck-Holtzhauer Y. Comparison of cytotoxicity of various surfactants tested on normal human fibroblast cultures using the neutral red test, MTT assay and LDH release. *J Appl Toxicol* 1999;**19**:163–165.
46. Chung TW, Moon SK, Chang YC, et al. Novel and therapeutic effect of caffeic acid and caffeic acid phenyl ester on hepatocarcinoma cells: complete regression of hepatoma growth and metastasis by dual mechanism. *FASEB J* 2004;**18**:1670–1681.
47. Tian X, Wong W, Xu A, et al. Uncoupling protein-2 protects endothelial function in diet-induced obese mice. *Circ Res* 2012;**110**:1211–1216.
48. Li N, Venkatesan MI, Miguel A, et al. Induction of heme oxygenase-1 expression in macrophages by diesel exhaust particle chemicals and quinones via the antioxidant-responsive element. *J Immunol* 2000;**165**:3393–3401.
49. Tan S, Sagara Y, Liu Y, Maher P, Schubert D. The regulation of reactive oxygen species production during programmed cell death. *J Cell Biol* 1998;**141**:1423–1432.
50. Herrera F, Martin V, Garcia-Santos G, et al. Melatonin prevents glutamate-induced oxytosis in the HT22 mouse hippocampal cell line through an antioxidant effect specifically targeting mitochondria. *J Neurochem* 2007;**100**:736–746.
51. Cho N, Choi JH, Yang H, et al. Neuroprotective and anti-inflammatory effects of flavonoids isolated from Rhus verniciflua in neuronal HT22 and microglial BV2 cell lines. *Food Chem Toxicol* 2012;**50**:1940–1945.
52. Sheng B, Wang X, Su B, et al. Impaired mitochondrial biogenesis contributes to mitochondrial dysfunction in Alzheimer's disease. *J Neurochem* 2012;**120**:419–429.
53. Gao X, Zheng CY, Qin GW, Tang XC, Zhang HY. S-52, a novel nootropic compound, protects against beta-amyloid induced neuronal injury by attenuating mitochondrial dysfunction. *J Neurosci Res* 2012;**90**:1981–1988.
54. Schaffer S, Asseburg H, Kuntz S, Muller WE, Eckert GP. Effects of polyphenols on brain ageing and Alzheimer's disease: focus on mitochondria. *Mol Neurobiol* 2012;**46**:161–178.
55. Lewerenz J, Letz J, Methner A. Activation of stimulatory heterotrimeric G proteins increases glutathione and protects neuronal cells against oxidative stress. *J Neurochem* 2003;**87**:522–531.
56. Salinas M, Wang J, Rosa de Sagarra M, et al. Protein kinase Akt/PKB phosphorylates heme oxygenase-1 *in vitro* and *in vivo*. *FEBS Lett* 2004;**578**:90–94.
57. Shibahara S, Han F, Li B, Takeda K. Hypoxia and heme oxygenases: oxygen sensing and regulation of expression. *Antioxid Redox Signal* 2007;**9**:2209–2225.
58. de Vries HE, Witte M, Hondius D, et al. Nrf2-induced antioxidant protection: a promising target to counteract ROS-mediated damage in neurodegenerative disease? *Free Radic Biol Med* 2008;**45**:1375–1383.
59. Kanninen K, Heikkinen R, Malm T, et al. Intrahippocampal injection of a lentiviral vector expressing Nrf2 improves spatial learning in a mouse model of Alzheimer's disease. *Proc Natl Acad Sci USA* 2009;**106**:16505–16510.
60. Wruck CJ, Gotz ME, Herdegen T, et al. Kavalactones protect neural cells against amyloid beta peptide-induced neurotoxicity via extracellular signal-regulated kinase 1/2-dependent nuclear factor erythroid 2-related factor 2 activation. *Mol Pharmacol* 2008;**73**:1785–1795.
61. Paupe V, Dassa EP, Goncalves S, et al. Impaired nuclear Nrf2 translocation undermines the oxidative stress response in Friedreich ataxia. *PLoS ONE* 2009;**4**:e4253.
62. Lo SC, Li X, Henzl MT, Beamer LJ, Hannink M. Structure of the Keap1:Nrf2 interface provides mechanistic insight into Nrf2 signaling. *EMBO J* 2006;**25**:3605–3617.
63. Linker RA, Lee DH, Ryan S, et al. Fumaric acid esters exert neuroprotective effects in neuroinflammation via activation of the Nrf2 antioxidant pathway. *Brain* 2011;**134**:678–692.